

Effect of Different Additives on the Size Control and Emission Properties of $\text{Y}_2\text{O}_3:\text{Eu}^{3+}$ Nanoparticles Prepared through the Coprecipitation Method

Abhijit P. Jadhav, Amol Pawar, Chang Woo Kim, Hyun Gil Cha, U. Pal,[†] and Young Soo Kang*

Department of Chemistry, Sogang University, Seoul 121-742, Republic of Korea

Received: June 25, 2009; Revised Manuscript Received: August 10, 2009

Nanoparticles of europium doped yttrium oxide ($\text{Y}_2\text{O}_3:\text{Eu}^{3+}$) were synthesized by the coprecipitation method using oleic acid as a surfactant in the presence of other additives. Incorporation of additives like ethylenediaminetetraacetic acid (EDTA) and NaCl in the reaction mixture drastically affects the particle size, size homogeneity, and emission behavior of the nanophosphors. Photoluminescence emission of the nanophosphors drastically enhances and quenches on addition of NaCl and EDTA in the reaction mixture, respectively. Such emission behaviors of the nanophosphors are explained considering the nephelauxetic effect induced by the incorporated ions in the reaction solution.

Introduction

Europium doped Y_2O_3 is a common luminescent material used in display technology. Compared with other metal oxide phosphors, $\text{Y}_2\text{O}_3:\text{Eu}^{3+}$ has added advantages for display applications such as short decay time, high quantum efficiency, good color coordination, and excellent material stability.¹ On the other hand, the particle size of the phosphors plays an important role on the image resolution of a cathode-ray display tube. For the same reason, the conventional phosphors of micrometer dimensions (1–10 μm) were replaced by nanometric phosphor particles to increase the image definition of CRT screens of color televisions.² The small phosphor particles of smooth spherical surface and narrow size distribution are ideal for this purpose, as they offer brighter cathodoluminescence performance of high definition due to high packing density and lower light scattering.^{3,4} Obtaining $\text{Y}_2\text{O}_3:\text{Eu}^{3+}$ nanoparticles of small diameter and narrow size distribution is a challenge for their efficient application in display technologies.

Synthesis of $\text{Y}_2\text{O}_3:\text{Eu}^{3+}$ nanoparticles has been reported using various methods such as combustion synthesis,^{5–7} the sol–gel method,⁸ microemulsions,⁹ chemical vapor deposition,¹⁰ spray pyrolysis,¹ and the hydrothermal¹¹ and coprecipitation methods.² By adequate control of the synthesis parameters, all of those techniques can produce more or less homogeneous nanoparticles of single phase, with uniform shape and acceptable microstructural uniformity.^{12–14} In general, the physical or solid state reaction syntheses of $\text{Y}_2\text{O}_3:\text{Eu}^{3+}$ nanostructures are performed at temperatures as high as 1500 °C with prolonged synthesis time. Sometimes such high temperature treatments cause the decrease of emission efficiency of the phosphors.¹⁵ On the other hand, a chemical technique like coprecipitation synthesis is simple, which involves dissolution of precursor compounds in water and subsequent precipitation of the reaction product through pH adjustment at relatively low or even at room temperature. However, to induce crystallization, the materials obtained through coprecipitation are fired at high temperatures.¹⁶

Generally, organic surfactants are used to control the grain growth and avoid agglomeration of nanoparticles in the chemical synthesis process. Surfactants reduce the oxygen bridge bonds between particles, avoiding their agglomeration tendency.² Apart from the surfactants, chelating agents are also used in the coprecipitation process, which act as binding agents. Chelating agents like tartaric acid,¹⁷ citric acid,^{18–20} and ethylenediaminetetraacetic acid (EDTA)^{21–23} have been used by several research groups for the synthesis of $\text{Y}_2\text{O}_3:\text{Eu}^{3+}$ nanoparticles. It is believed that EDTA has a greater ability to chelate metal cations and forms very stable and soluble complexes.

When a metal ion is surrounded by ligands in a complex, the ligand orbitals directed toward the metal ion produce changes in its total electronic environment. When a ligand is bound to a metal ion, the orbitals on the metal ion are smeared out over a larger space. The molecular orbital terminology for this situation is that the electrons become more delocalized in the complex than they are in the free ion. Such expansion of the electron cloud is known as the nephelauxetic effect.²⁴

When the solar energy passes through the atmosphere, a number of phenomena take place. A portion of the energy is reflected or scattered back to the space by clouds and other atmospheric particles. Some part of energy is absorbed by atmospheric gases like ozone. Most of the energy passing through the earth's atmosphere is utilized by plants for photosynthesis and for heating the earth's surface. Thus, conversion of the UV portion of the solar spectrum into visible and near IR is essential for better utilization of energy.

The ultraviolet portion of the sunlight reaching the earth's surface is less intense than other portions of the spectrum. It was observed that harmful insects do not prefer to live in the greenhouse environment where UV light is blocked or filtered. The insects like cockroaches, aphids, and vermins are phototaxis to the ultraviolet light. Thus, wavelength conversion has been of dual advantage for energy utilization and insect control.²⁵

In the present article, we report on the synthesis of $\text{Y}_2\text{O}_3:\text{Eu}^{3+}$ nanoparticles using oleic acid as surfactant and additives like EDTA and NaCl. The effect of those additives on the size and composition control and photoluminescence emission characteristics of the nanophosphors have been studied. The results were compared with $\text{Y}_2\text{O}_3:\text{Eu}^{3+}$ synthesized without

* Corresponding author. Phone: + 82 2 705 8882. Fax: + 82 2 701 0967. E-mail: yskang@sogang.ac.kr.

[†] On leave from Instituto de Física, Universidad Autónoma de Puebla, México.

using surfactant. The obtained results indicate that the addition of additives helps one to obtain nanophosphors with a narrow size distribution. It has been demonstrated that the presence of NaCl with oleic acid enhances the photoluminescence (PL) intensity of the Y₂O₃:Eu³⁺ nanophosphors, while addition of EDTA along with oleic acid quenches emission. Y₂O₃:Eu³⁺ nanoparticles synthesized without surfactant have a wide size distribution, as there was no control over their growth.

Experimental Section

Materials. Yttrium oxide (Y₂O₃, 99.99%, Sigma Aldrich), europium oxide (Eu₂O₃, 99.9%, Sigma Aldrich), sodium carbonate (Na₂CO₃, Junsei Chemicals Co. Ltd.), sodium chloride (NaCl, Duksan Pure Chemical Co. Ltd.), oleic acid (C₁₈H₃₄O₂, Junsei Chemicals Co. Ltd.), hydrochloric acid (HCl, Jin Chemicals Pharmaceuticals Co. Ltd.), and ethylenediaminetetraacetic acid (C₁₀H₁₆N₂O₈, Junsei Chemicals Co. Ltd.) were used as received without further purification.

Synthesis. The synthesis of Y₂O₃:Eu³⁺ nanoparticles was carried out by the coprecipitation method.²⁶ In a typical coprecipitation process, 95.0 mmol of YCl₃·6H₂O (0.725 g) and 5.0 mmol of EuCl₃·6H₂O (0.05 g) were mixed in 50.0 mL of deionized (DI) water along with 1.0 mL of surfactant under vigorous magnetic stirring for 2 h. While using NaCl with oleic acid as the surfactant, 0.436 g (7.46 mmol) of NaCl was added into the reaction mixture. In the case of Y₂O₃:Eu³⁺ nanostructures synthesized using oleic acid and EDTA, 0.02 g (2.0 mmol) of EDTA was added to the reaction mixture. The precipitation of the complex oxalate from the solution was carried out by dropwise addition of an aqueous Na₂CO₃ solution (0.3 × 10⁻³ M), maintaining the final pH at 7.0. A white precipitate was formed on addition of the Na₂CO₃ solution. The obtained product was washed repeatedly with DI water and separated by filtration. The as-prepared samples were dried at 80 °C for 6 h in ambient air and then annealed in air at 800 °C for 1 h using a muffle furnace.

Characterizations. The size and shape of the synthesized nanoparticles were examined using JEOL, JEM-2010, and JEOL JEM 2100F transmission electron microscopes operating at 200 kV. For transmission electron microscopy (TEM) observations, a small amount of the powder sample was dispersed into cyclohexane and a drop of it was placed over a carbon coated microscopic copper grid (300 mesh size). The TEM grid was then dried under an UV lamp. The particle's surface element binding energy and surface composition were characterized by a Thermo VG Scientific (England), Multitab 2000 X-ray photoelectron spectrometer. The powder X-ray diffraction (XRD) patterns of the as-prepared and annealed samples were recorded using the Cu K α radiation ($\lambda = 1.54056 \text{ \AA}$) of a Rigaku X-ray diffractometer operating at 40 kV and 150 mA at a scanning rate of 0.02° per step in the 2 θ range of 10° ≤ 2 θ ≤ 80°. The UV–vis optical absorbance of the nanoparticles was measured using an Agilent 8453 spectrometer. The room temperature PL of the powder samples was measured using a Hitachi F-7000 fluorescence spectrophotometer using the 265 nm excitation of a xenon lamp.

Result and Discussion

The XRD patterns of Y₂O₃:Eu³⁺ nanoparticles synthesized using oleic acid with different additives and annealed at 800 °C are shown in Figure 1. The results were compared with Y₂O₃:Eu³⁺ synthesized without using surfactant. The diffraction peaks appearing at 2 θ = 20.6, 29.2, 31.5, 33.8, 48.5, 57.6, and 78.8° correspond to the (211), (222), (321), (400), (440), (622), and

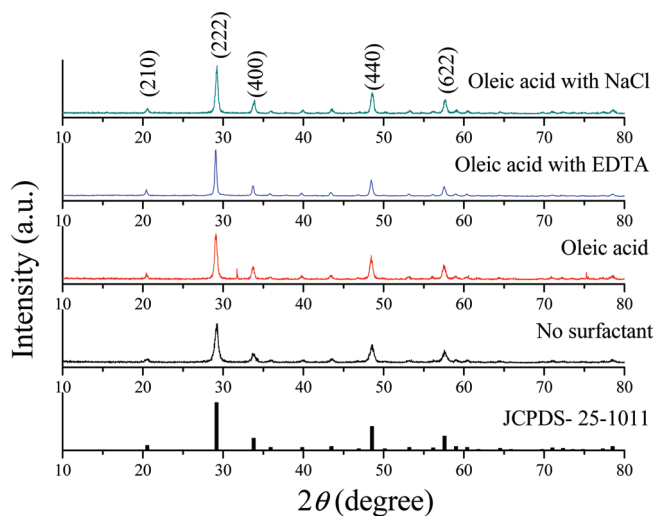


Figure 1. XRD spectra of the Y₂O₃:Eu³⁺ nanoparticles synthesized using oleic acid, oleic acid with EDTA, oleic acid with NaCl, and without using surfactant. The phosphor samples were annealed at 800 °C for 1 h in air.

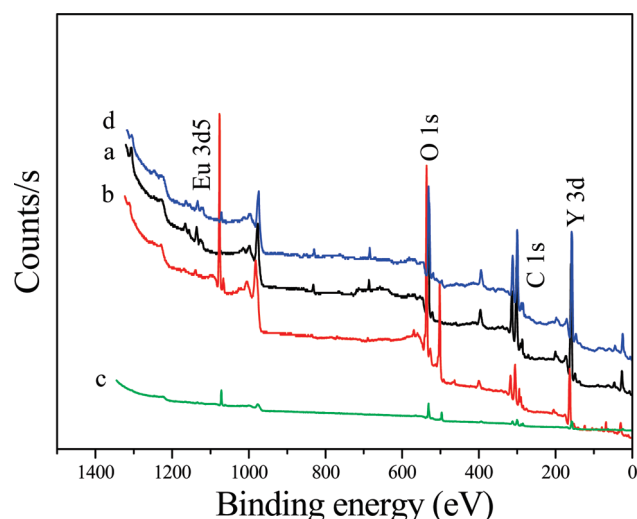


Figure 2. XPS survey spectra of the Y₂O₃:Eu³⁺ nanoparticles synthesized using (a) no surfactant, (b) oleic acid, (c) oleic acid and EDTA, and (d) oleic acid and NaCl.

(653) planes of the body centered cubic structure of Y₂O₃:Eu³⁺. The high intensity of the diffraction peaks indicates good crystallinity of the nanoparticles.

Figure 2 shows the comparative survey spectra of Y₂O₃:Eu³⁺ samples synthesized using oleic acid and other additives. The results were compared with Y₂O₃:Eu³⁺ synthesized without using surfactant. All of the XPS spectra revealed photoelectron peaks corresponding to Y, O, C, and Eu. The emission peak positions were corrected using the C1s peak position at 284.6 eV as a reference. This calibration was necessary, as the samples were of poor electrical conductivity, and hence, sample charging took place during analysis.²⁸ Table 1 presents the surface composition of Y₂O₃:Eu³⁺ nanoparticles synthesized using oleic acid and other additives. As can be seen in the table, though all of the samples were prepared with the same nominal concentration of Eu (Eu:O = 5:95), the atom % of Eu varied from sample to sample. The estimated Eu concentration was lowest for the sample prepared with oleic acid only and highest for the sample prepared without any surfactant or additive.

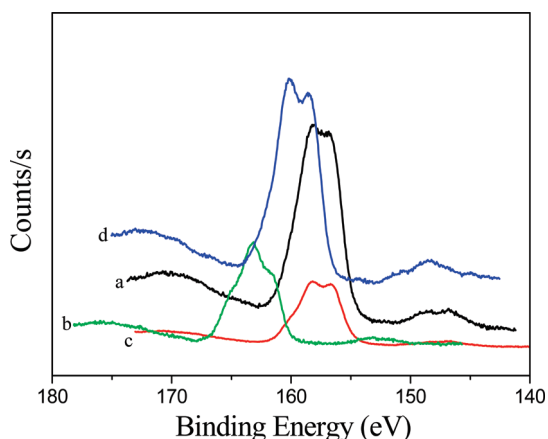
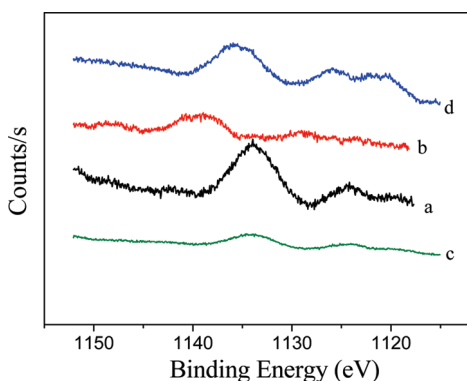
Figure 3 shows the XPS spectra of the samples in the Y3d emission region. The Y3d core level peak is split into two states,

TABLE 1: Composition of the $Y_2O_3:Eu^{3+}$ Nanoparticles Synthesized Using Oleic Acid and Different Additives Estimated through XPS Analysis

$Y_2O_3:Eu^{3+}$	Eu ³⁺ (atom %)	O (atom %)	Y (atom %)
no surfactant	0.80	65.63	33.57
oleic acid	0.23	84.45	15.52
oleic acid with EDTA	0.43	63.68	35.89
oleic acid with NaCl	0.49	64.41	35.10

viz., $Y3d_{5/2}$ and $Y3d_{3/2}$ as the result of spin-orbit coupling.^{27,28} The $Y3d_{5/2}$ and $Y3d_{3/2}$ peaks for the $Y_2O_3:Eu^{3+}$ sample synthesized without surfactant were located at about 156.8 and 158.3 eV, respectively. The position of the peaks positively shifted about 4.9 eV for the $Y_2O_3:Eu^{3+}$ nanoparticles prepared with oleic acid and about 1.8 eV for the sample prepared with oleic acid and NaCl. On the other hand, the peak positions did not change for the sample prepared using oleic acid and EDTA. Such a different chemical shift in different samples indicates the different order of bonding between the Y and O atoms²⁹ when they are synthesized with different additives.

The XPS emissions for the samples in the Eu($3d$) transition region are shown in Figure 4. The binding energy of the $Eu3d_{5/2}$ core level for bulk Eu_2O_3 is 1135.6 eV.³⁰ From Figure 4, we can calculate the difference in binding energy of the $Eu3d_{5/2}$ level for the samples prepared using different additives to have an idea of their chemical environments. The estimated binding energies of the $Eu3d_{5/2}$ level for $Y_2O_3:Eu^{3+}$ synthesized using no surfactant, oleic acid, oleic acid with EDTA, and oleic acid

**Figure 3.** Comparison of the $Y3d$ emission bands for the $Y_2O_3:Eu^{3+}$ nanoparticles synthesized using (a) no surfactant, (b) oleic acid, (c) oleic acid with EDTA, and (d) oleic acid with NaCl.**Figure 4.** Comparison of the $Eu3d_5$ emission bands for the $Y_2O_3:Eu^{3+}$ nanoparticles synthesized using (a) no surfactant, (b) oleic acid, (c) oleic acid and EDTA, and (d) oleic acid with NaCl.

with NaCl were 1133.94, 1139.01, 1133.87, and 1135.54 eV, respectively. It can be observed that the chemical shift of the $Eu3d_{5/2}$ band is least for the sample prepared with oleic acid and NaCl (−0.06 eV) from its standard value (1135.6 eV), which indicates the Eu^{3+} ions occupying Y^{3+} sites in the Y_2O_3 lattice. The higher chemical shift for the $Y_2O_3:Eu^{3+}$ samples synthesized using no surfactant, oleic acid, and oleic acid with EDTA indicates the Eu^{3+} ion in them occupied interstitial sites of the Y_2O_3 lattice.³⁰

Figure 5 shows the typical TEM images of $Y_2O_3:Eu^{3+}$ nanoparticles synthesized using (a) no surfactant, (b) oleic acid, (c) oleic acid with EDTA, and (d) oleic acid with NaCl, respectively. Formation of nanoparticles in all of the samples is clear from their corresponding images. The lack of surfactant results in irregular particle shape and size (Figure 5a) of the nanoparticles with frequent agglomeration, as there was no control over growth of precipitating particles. The nanoparticles of sizes ranging from 12 to 28 nm (average size 21 nm) were formed for the sample prepared without using surfactant. Nanoparticles of size ranging from 100 to 120 nm (average size 129 nm) were formed (Figure 5b) for the sample synthesized using oleic acid surfactant. The particles in this case were also frequently agglomerated. Colloidal chemistry plays a significant role in the precipitation of powders from solution. In chemical coprecipitation, the main controlling factor that causes high agglomeration of individual particles is the interparticle force.³¹ The rate of agglomeration is largely dependent on the rate of particle collision per unit time. These collisions are caused by Brownian motion, thermal convection, and shear forces. Shear forces caused by stirring is the main source of collision in the coprecipitation process. The balance of these forces determines whether particles adhere once they come into contact. If there is a net attractive force, the particles will bond to form an agglomerate.³² Addition of a chelating agent like EDTA produces a nanoparticle of about 18 nm average size (Figure 5c). Addition of EDTA helps to form stable soluble complexes with metals. EDTA anions have a greater ability to chelate metal cations, which helps to form nanoparticles of narrow size distribution (Figure 5c). Figure 5d shows a typical TEM image of the $Y_2O_3:Eu^{3+}$ sample synthesized using oleic acid and NaCl. The image clearly shows that addition of NaCl along with oleic acid helped to form uniform nanoparticles of about 21 nm average size. The adsorption of NaCl over precipitating nanoparticles restricts their growth and suppresses their agglomeration.

Room temperature PL spectra of $Y_2O_3:Eu^{3+}$ nanoparticles synthesized using oleic acid and different additives recorded under $\lambda_{exc} = 265$ nm are shown in Figure 6. The host Y_2O_3 crystal has a cubic unit cell structure with space group $Ia\bar{3}$, where $3/4$ Y^{3+} occupies the low symmetric C_2 site and $1/4$ Y^{3+} occupies the high symmetric S_6 site. The activator Eu^{3+} ions display two typical luminescence emissions, one due to the $^5D_0 \rightarrow ^7F_2$ transition at about 614 nm and the other related to the $^5D_0 \rightarrow ^7F_1$ transition around 594 nm. If Eu^{3+} ions in the host dominantly occupy the site with low symmetry, the selection rule will partially be broken, and the emission at about 614 nm will be strengthened greatly, while the 594 nm transition would be weakened remarkably.^{33–38} The weaker shoulder peak appearing at about 630 nm corresponds to the $^5D_0 \rightarrow ^7F_3$ transition. The PL spectrum of our $Y_2O_3:Eu^{3+}$ nanoparticles synthesized using oleic acid and NaCl shows maximum luminescence intensity, which is contrary to the observation of Huang Yan, who has reported a slight decrease of emission intensity on the addition of NaCl in the reaction solution.³⁹ The most intense peak associated with the $^5D_0 \rightarrow ^7F_2$ transition for

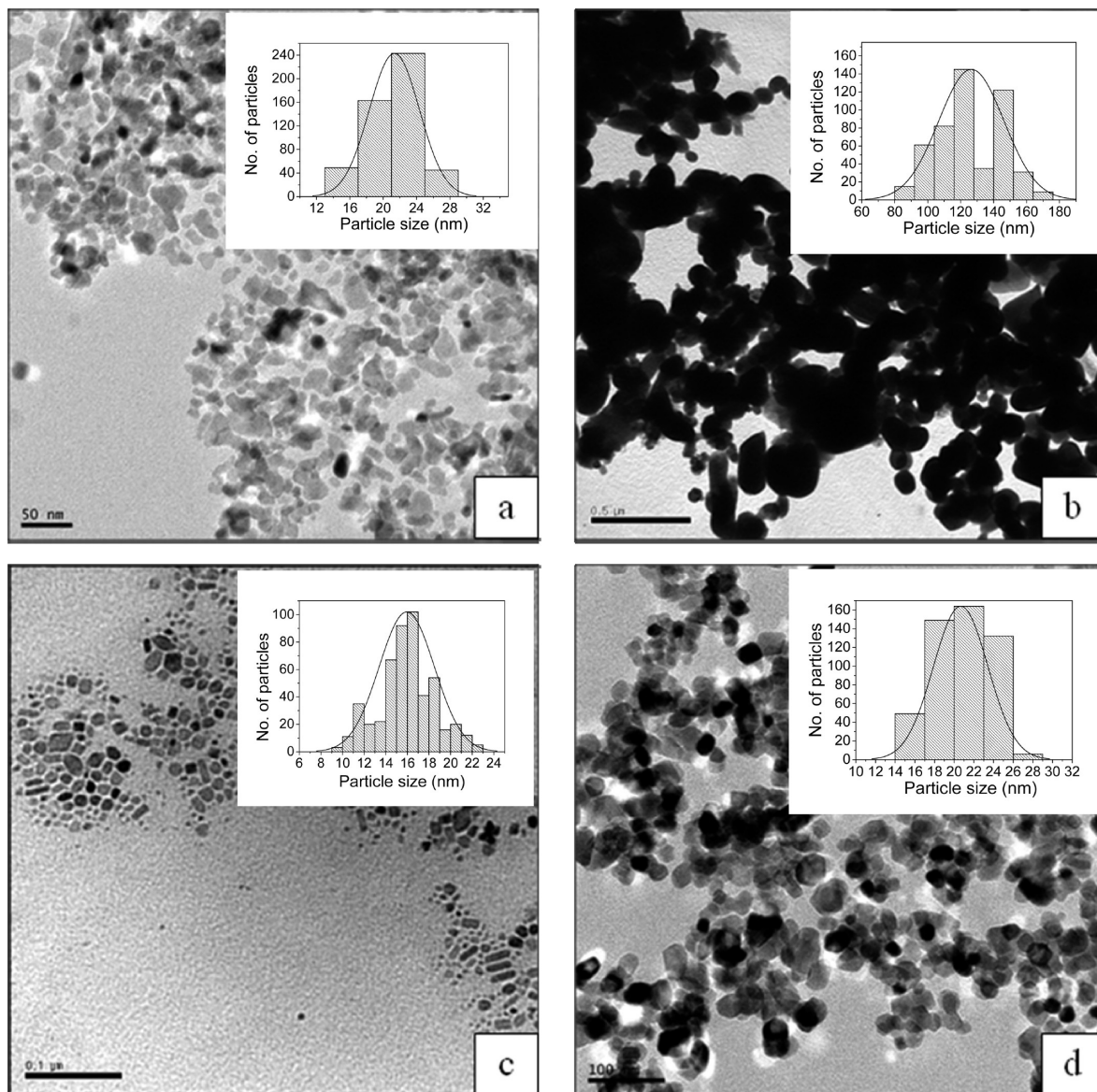


Figure 5. Typical TEM images of the Y₂O₃:Eu³⁺ nanoparticles synthesized using (a) no surfactant, (b) oleic acid, (c) oleic acid with EDTA, and (d) oleic acid with NaCl. All of the samples were annealed at 800 °C in air for 1 h. Corresponding size distribution histograms are presented as insets.

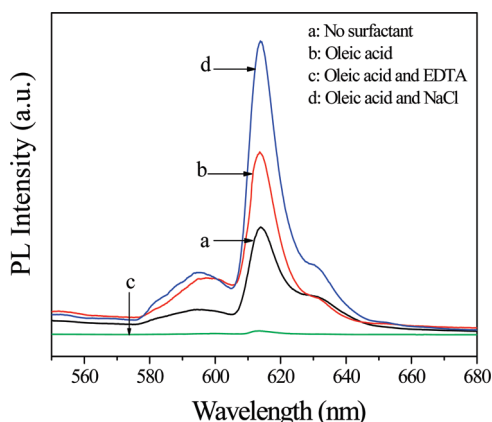


Figure 6. Room temperature PL spectra of the Y₂O₃:Eu³⁺ nanoparticles synthesized using (a) no surfactant, (b) oleic acid, (c) oleic acid with EDTA, and (d) oleic acid with NaCl. For excitation, 265 nm emission of a xenon lamp was used.

the sample prepared with oleic acid was observed at about 613.6 nm. Addition of EDTA along with oleic acid results in a mild

TABLE 2: Variation of PL Intensity Variation at Room Temperature for the Y₂O₃:Eu³⁺ Nanoparticles Synthesized Using Oleic Acid and Other Additives

surfactants	particle size (nm)	intensity of the 614 nm PL band (a.u.)
no surfactant	21.34	5296.77
oleic acid	126.50	7721.6
oleic acid with EDTA	15.95	175.65
oleic acid with NaCl	20.66	23396.00

blue-shift of the emission band to 613.4 nm, while the addition of NaCl along with oleic acid causes a mild red-shift of the band to 613.8 nm. The change in the position of the most intense peak is related to the nephelauxetic effect, which is generally ascribed to the covalency contribution of the ligands in the first coordination shell of the central ion via the phenomenological equation of Frey and Horrocks.^{40,41} The intensities of the most intense emission peak of the Y₂O₃:Eu³⁺ nanoparticles synthesized using different additives are presented in Table 2. While the PL intensity for the Y₂O₃:Eu³⁺ nanoparticles prepared using oleic acid and NaCl was the highest, the emission for the sample

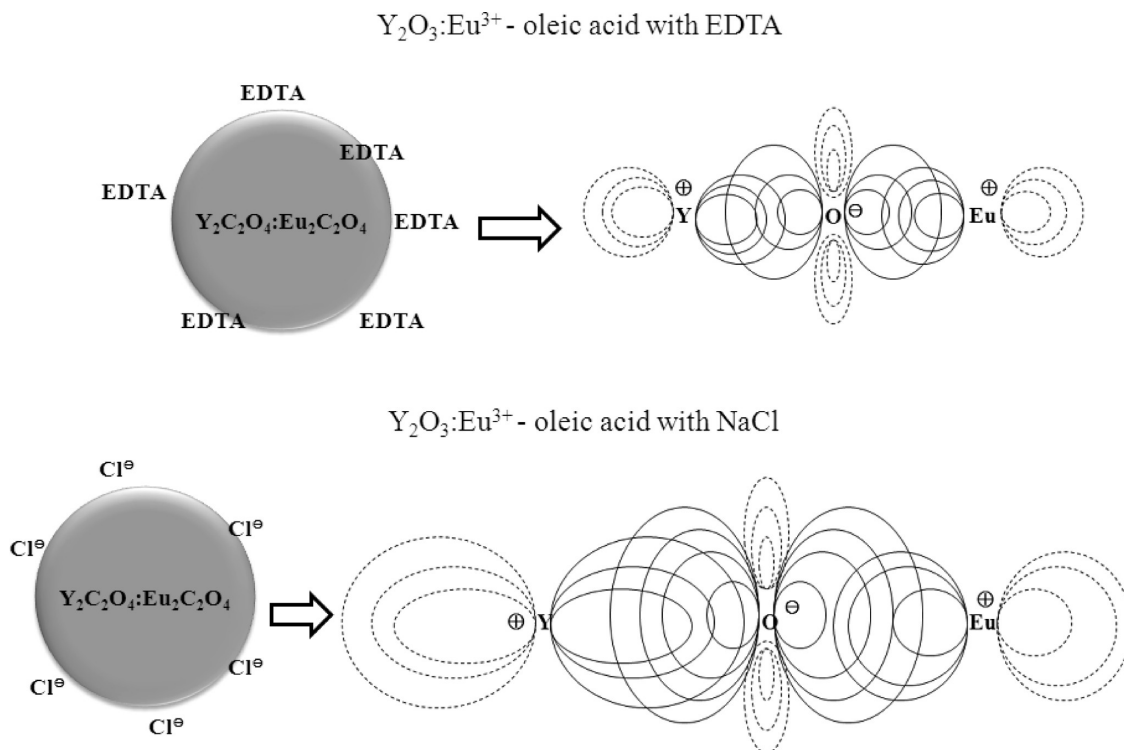


Figure 7. Illustration of electron cloud increase due to the nephelauxetic effect in $Y_2O_3:Eu^{3+}$ synthesized using oleic acid with EDTA and oleic acid with NaCl.

prepared using oleic acid and EDTA was the lowest. Such a variation of emission intensity in the $Y_2O_3:Eu^{3+}$ nanoparticles synthesized with different additives could be understood considering the nephelauxetic effect.⁴² It is a decrease of interelectronic repulsion between the valence electrons of an ion in a host crystal in comparison with its value when the ion is free, due to covalency of the bonds between the central ion and ligands.⁴³ Oleic acid is insoluble in water. It has a polar hydrophilic headgroup and a nonpolar hydrophobic tail. The surface tension of oleic acid tends to form micelles as molecular aggregates. As the precipitation process starts, the nanoparticles start growing at the surface of the micellar globe. After removal of solvent through a centrifuging process, nanoparticles covered with oleic acid are obtained. The organic part (surfactant) is removed during the calcination process, and monodispersed nanoparticles are obtained.

The homogeneous distribution of Eu^{3+} within the host lattice helps to determine interatomic distances of adjacent Eu^{3+} ions.⁴⁴ The atomic radius of europium is higher than that of the yttrium atom. Thus, at higher temperature, segregation of europium atoms takes place and some dopant europium may escape from the lattice site, causing a decrease in luminescence quenching. However, addition of EDTA and NaCl has a different effect on the optical properties of $Y_2O_3:Eu^{3+}$. Y and Eu ions can chelate with EDTA and form stable complexes at pH 7.0. At this pH value, EDTA can bind to the yttrium rich Y_2O_3 and chelate with free europium ions as well. The EDTA molecule has six binding sites which include four COO^- carboxylic groups and two single pairs of electrons on nitrogen. When a single EDTA molecule chelates with Y or Eu ion, all of its six binding sites participate in the reaction. The EDTA molecule chelates with yttrium ion on the Y_2O_3 surface, and it is possible that all six bonding sites of EDTA participate in bond formation. Consequently, two adjacent outward sides of two EDTA molecules can be used to chelate with a free Eu^{3+} ion.⁴⁵

Addition of NaCl plays an important role in controlling the particle size of the $Y_2O_3:Eu^{3+}$ nanophosphor. As has been observed from the TEM micrographs, addition of NaCl along with oleic acid produces $Y_2O_3:Eu^{3+}$ nanoparticles with narrow particle size distribution. The dissolved salt forms an adsorbed layer over the surface of the precipitating nanoparticles. This adsorbed layer restricts the growth of nanoparticles, avoiding their agglomeration.^{46–48} It has been reported that the Na^+ and Cl^- ions form the double electric layer at the liquid membranes over the nanoparticles, preventing their further growth.⁴⁹ As NaCl has good solubility in water, it can be removed easily by washing the samples in water, rendering no possibility of contamination. As has been mentioned earlier, addition of NaCl also increased the PL intensity of our $Y_2O_3:Eu^{3+}$ nanophosphors. We believe that the addition of NaCl in the reaction mixture helps to promote the diffusion of Y^{3+} and Eu^{3+} during the growth of $Y_2O_3:Eu^{3+}$ nanoparticles, which in turn helps to maintain the homogeneous distribution of Eu^{3+} ions in the samples, promoting higher crystallization degree and reducing surface defects. As can be seen from Figure 6 and Table 2, addition of NaCl in the reaction mixture enhanced the PL intensity of the nanoparticles about 2 times in comparison with the nanoparticles prepared only with oleic acid.

The nephelauxetic effect depends upon the nature of complexing ligands and can be understood by a nephelauxetic series of ligands: $F^- < H_2O < tart^{2-} < bac^- < EDTA^{4-} < bipy < Phen < Cl^- < Br^- < I^- < O^{2-}$.⁵⁰ In this series, the nephelauxetic effect increases from F^- to O^{2-} ions. The increase in the electron cloud is supposed to be responsible for the increase of the orbital size of the ions (Figure 7). The variation of PL intensity in the nanoparticles is directly related to the nephelauxetic effect, as due to the expansion of the electron cloud the bond length of $Eu-O$ changes.⁴² Since the Cl^- ligand induces a higher nephelauxetic effect than the $EDTA^{4-}$ ligand, its electron cloud is large in size as compared to the case of the EDTA ligand,

hence a higher orbital size. The electronic configuration of europium is [Xe] 4f⁷ 6s², and the PL emission in Y₂O₃:Eu³⁺ is the result of the transition between *d* and *f* energy levels. The intense emission peak at 614 nm is the result of the transition ⁵D₀ → ⁷F₂. Due to the nephelauxetic effect, the effective positive charge on the metal gets reduced due to the negative charge of the ligand,⁴³ resulting in slight expansion of the *f* orbital, causing an enhancement of luminescence emission intensity, as in the case of Y₂O₃:Eu³⁺ nanoparticles synthesized using oleic acid and NaCl.

Conclusion

In summary, Y₂O₃:Eu³⁺ nanophosphors were synthesized using oleic acid surfactant and other additives like EDTA and NaCl. The well crystalline nanoparticles show a great effect of the additives on their room temperature PL emissions. Y₂O₃:Eu³⁺ nanoparticles synthesized using oleic acid and NaCl together were of most uniform size with highest emission efficiency. Addition of NaCl or EDTA along with oleic acid improves the size homogeneity and reduces surface defects of Y₂O₃:Eu³⁺ nanoparticles. We have demonstrated that the red emitting Y₂O₃:Eu³⁺ nanophosphors of about 20 nm average size and of high PL emission intensity can be prepared using a suitable surfactant such as oleic acid and NaCl as an additive in the coprecipitation method. Addition of additives like NaCl in the reaction solution in the presence of oleic acid induces the nephelauxetic effect, causing expansion of the *f* orbital which is responsible for the PL emission enhancement in the nanostructures.

Acknowledgment. This work was financially supported by Energy Technology Research and Development 2008 and the Brain Korea 21.

References and Notes

- Joffin, N.; Dexpert-Ghys, J.; Verelst, M.; Baret, G.; Garcia, A. *J. Lumin.* **2005**, *113*, 249.
- He, C.; Guan, Y.; Yao, L.; Cai, W.; Yao, Z. *Mater. Res. Bull.* **2003**, *38*, 973–979.
- Martinez-Rubio, M. I.; Ireland, T. G.; Fern, G. R.; Silver, J.; Snowden, M. J. *Langmuir* **2001**, *17*, 7145.
- (a) Vecht, A.; Gibbons, C.; Davies, D. *J. Vac. Sci. Technol., B* **1999**, *17*, 750. (b) Jing, X.; Ireland, T. G.; Gibbons, C.; Barber, D. J.; Silver, J.; Vecht, A.; Fern, G.; Trogwa, P.; Morton, D. *J. Electrochem. Soc.* **1999**, *146*, 4546. (c) Jiang, Y. D.; Wang, Z. L.; Zhang, F.; Paris, H. G.; Summers, C. J. *J. Mater. Res.* **1998**, *13*, 2950. (d) Bechtel, H.; Nikol, H. *Proc. Electrochem. Soc.* **1998**, *97*, 256.
- Fu, Z.; Zhou, S.; Pan, T.; Zhang, S. *J. Lumin.* **2007**, *124*, 213–216.
- Zhang, W. W.; Zhang, W. P.; Xie, P. B.; Yin, M.; Chen, H. T.; Jing, L.; Zhang, Y. S.; Lou, L. R.; Xia, S. D. *J. Colloid Interface Sci.* **2003**, *262*, 588.
- Wang, J. W.; Chang, Y. M.; Chang, H. C.; Lin, S. H.; Huang, L. C. L.; Kong, X. L.; Kang, M. W. *Chem. Phys. Lett.* **2005**, *405*, 314.
- Sharma, P. K.; Nass, R.; Schmidt, H. *Opt. Mater.* **1998**, *10*, 161.
- Huang, H.; Xu, G. Q.; Chin, W. S.; Gan, L. M.; Chew, C. H. *Nanotechnology* **2002**, *13*, 318.
- Konrad, A.; Fries, T.; Gahn, A.; Kummer, F.; Herr, U.; Tidecks, R.; Samwer, K. *J. Appl. Phys.* **1999**, *86*, 3129.
- Bai, X.; Song, H.; Yu, L.; Yang, L.; Liu, Z.; Pan, G.; Lu, S.; Ren, X.; Lei, Y.; Fan, L. *J. Phys. Chem. B* **2005**, *109*, 15236–15242.
- (a) Zhou, Y. H.; Lin, J.; Yu, M.; Han, S. M.; Wang, S. B.; Zhang, H. *J. Mater. Res. Bull.* **2003**, *38*, 1289. (b) Wang, L. S.; Zhou, Y. H.; Quan, Z. W.; Lin, J. *Mater. Lett.* **2005**, *59*, 1130.
- Wakefield, G.; Holland, E.; Dobson, P. J.; Hutchison, J. L. *Adv. Mater. (Weinheim, Ger.)* **2001**, *13*, 1557.
- Sun, Y.; Qi, L.; Lee, M.; Samuels, W. D.; Exarhos, G. J. *J. Lumin.* **2004**, *109*, 85–91.

- (a) Zhou, Y. H.; Lin, J.; Yu, M.; Han, S. M.; Wang, S. B.; Zhang, H. *J. Mater. Res. Bull.* **2003**, *38*, 1289. (b) Wang, L. S.; Zhou, Y. H.; Quan, Z. W.; Lin, J. *Mater. Lett.* **2005**, *59*, 1130.
- Wakefield, G.; Holland, E.; Dobson, P. G.; Hutchison, J. L. *Adv. Mater. (Weinheim, Ger.)* **2001**, *13*, 1557.
- Sun, Y.; Qi, L.; Lee, M.; Samuels, W. D.; Exarhos, G. J. *J. Lumin.* **2004**, *109*, 85–91.
- Taxak, V. B.; Khatkar, S. P.; Han, S. D.; Kumar, R.; Kumar, M. J. *Alloys Compd.* **2009**, *469*, 224–228.
- Ferrari, J. L.; Pires, A. M.; Davolos, M. R. *J. Mater. Chem. Phys.* **2009**, *113*, 587–590.
- Pang, M. L.; Lin, J.; Cheng, Z. Y.; Fu, J.; Xing, R. B.; Wang, S. B. *Mater. Sci. Eng., B* **2003**, *100*, 124–131.
- Pechini, M. P. U.S. Patent 3 330 697, 1967.
- Zhang, J.; Zhang, Z.; Tang, Z.; Lin, Y.; Zheng, Z. *J. Mater. Proc. Technol.* **2002**, *121*, 265.
- Zhang, J.; Tang, Z.; Zhang, Z.; Fu, W.; Wang, J.; Lin, Y. *Mater. Sci. Eng., A* **2002**, *334*, 246.
- Lian, S.; Rong, C.; Yin, D.; Liu, S. *J. Phys. Chem. C* **2009**, *113*, 6298–6302.
- House, J. E. *Inorganic Chemistry*; Elsevier publications, Canada, Academic Press, 2008; p 655.
- Jadhav, A. P.; Kim, C. W.; Cha, H. G.; Pawar, A.; Jadhav, N.; Pal, U.; Kang, Y. S. *J. Phys. Chem. C* **2009**, *113*, 13600–13604.
- Small, D. M. *J. Am. Oil Chem. Soc.* **1968**, *45*, 3, 108–119.
- Yang, L.; Tang, Y.; Chen, X.; Li, Y.; Cao, X. *Mater. Chem. Phys.* **2007**, *101*, 195–198.
- Ingo, G. M.; Marletta, G. *Nucl. Instrum. Methods Phys. Res., Sect. B* **1996**, *116*, 440.
- Duraud, J. P.; Jollet, F.; Thomat, N.; Gautier, M.; Maire, P.; le Gressus, C.; Dartyge, E. *J. Am. Ceram. Soc.* **1990**, *73*, 2467.
- Pol, V. G.; Reissfeld, R.; Gedanken, A. *Chem. Mater.* **2002**, *14*, 3920–3924.
- Yang, L.; Tang, Y.; Chen, X.; Li, Y.; Cao, X. *Mater. Chem. Phys.* **2007**, *101*, 195–198.
- Sheen, S. R.; Chen, D. H.; Hsu, B. F.; Chang, C. T.; Shei, C. Y.; Huang, J. C.; Sun, Y. L.; Sugimoto, T.; Matijevic, E. *J. Inorg. Nucl. Chem.* **1979**, *41*, 165.
- Wang, Z. L.; Liu, Y.; Zhang, Z. *Handbook of Nanophase and Nanostructured Materials*; Kluwer Academic/ Plenum Publishers, Tsinghua University Press; Vol. 1.
- Anh, V. N.; T. K.; Yi, G. C.; Streak, W. *J. Lumin.* **2007**, *122–123*, 776.
- Shionoya, S.; Yen, W. M.; Takashi, H. *Phosphor Handbook*; CRC Press: Boca Raton, FL, 1999; p 112.
- Butler, K. H. *Fluorescent Lamp Phosphors Technology and Theory*; University Park and London, The Pennsylvania State University Press, 1980; p 15.
- Wakefield, G.; Holland, E.; Dobson, P. J.; Hutchison, J. L. *Adv. Mater.* **2001**, *13* (20), 1557.
- Yu, Z.; Huang, X.; Zhuang, W.; Cui, X.; He, H.; Li, H. *J. Rare Earths* **2004**, *22* (6), 829.
- Tiseanu, C.; Parvulescu, V. I.; Kumke, M. U.; Dobroiu, S.; Gessner, A.; Simon, S. *J. Phys. Chem. C* **2009**, *113*, 5784–5791.
- Frey, S. T.; De, W.; Horrocks, W., Jr. *Inorg. Chim. Acta* **1995**, *229*, 383.
- Hirayama, M.; Sonoyama, N.; Yamada, A.; Kanno, R. *J. Solid State Chem.* **2009**, *182*, 730–735.
- Suchocki, A.; Biernacki, S. W.; Kaminska, A.; Arizmendi, L. *J. Lumin.* **2003**, *102–103*, 571–574.
- Shin, S. H.; Kang, J. H.; Jeon, D. Y.; Zang, D. S. *J. Lumin.* **2005**, *114* (3–4), 275.
- Yan, H.; Yunsheng, H.; Xiaoming, T.; Zhen, L.; Hongqi, Y.; Weidong, Z. *J. Rare Earths* **2007**, *25*, 697–700.
- Flaschka, H. A. *EDTA Titrations: An Introduction to Theory and Practice*; Oxford Pergamon Press: New York, 1964.
- Zhu, G.; Tomsia, K. D.; Yu, H.; Motlan, E. M.; Goldys, *Solid State Commun.* **2006**, *137*, 503–506.
- Yan, H.; Hongqi, Y.; Weidong, Z.; Yunsheng, H.; Chunlei, Z.; Cui, L.; Songxia, G. *Trans. Nonferrous Met. Soc. China* **2007**, *17*, 644–648.
- Jun, R.; Shouci, L.; Jian, S.; Boxing, H. *Chin. Sci. Bull.* **2000**, *45*, 1376–1380.
- Sastri, V. S. Bünzli, J.-C. G. Rao, V. R. Rayudu, G. V. S. Perumareddi, J. R. *Modern Aspects of Rare Earths and their Complexes*; Elsevier publications: 2003; p 592.